Int. J. Nanosci. Nanotechnol., Vol. 19, No. 2, June 2023, pp. 109-119
DOI: 10.22034/ijnn.2023.559299.2248

Dye Excitation and Surface Defects Mediated Photocatalytic Behavior of Vertically Aligned ZnO Nanorods

Sundara Venkatesh Perumalsamy[1,2,*], Prabhu Saravanan[3], Jothivenkatachalam Kandasamy[4] and Jeganathan Kulandaivel[2]

[1]Nanomaterials Laboratory, Department of Physics, Sri S. Ramasamy Naidu Memorial College, Sattur - 626 203, Tamil Nadu, India
[2]Centre for Nanoscience and Nanotechnology, Department of Physics, Bharathidasan University, Tiruchirappalli - 620 024, Tamil Nadu, India
[3]Department of Physical-Chemistry, Faculty of Chemical Sciences, University of Concepcion, Chile
[4]Department of Chemistry, Anna University, BIT Campus, Tiruchirappalli - 620 024, Tamil Nadu, India

(*) Corresponding author: srnmcphysics@gmail.com
(Received: 28 July 2022 and Accepted: 20 April 2023)

Abstract

Photocatalyst for the degradation of the organic dye molecules has been investigated for the highly uniform vertically aligned ZnO nanorods grown on silicon substrates by radio frequency magnetron sputtering. An intense green luminescence located at 2.192 eV is corroborated by the singly charged oxygen vacancies and it is responsible for the visible-light-driven photocatalytic response in ZnO nanorods. The higher photocatalytic activity of organic dyes under the irradiation of visible light is enhanced due to the light absorption and better charge separation (e^--h^+) in vertically aligned ZnO nanorods. Further, the dye excitation is also accountable for the degradation mechanism besides surface defects under solar irradiation. Moreover, the ZnO nanorods exhibit suppressed photo corrosion and high photo-stability as evidenced by the recovery and recycling studies.

Keywords: *ZnO nanorods, Sputtering, Photoluminescence, Dye molecules, Photodegradation.*

1. INRODUCTION

Materials having photocatalytic behavior with non-toxic nature are received enormous research interest in the field of catalysis in recent times [1-3]. In photocatalytic dye degradation, the materials have been illuminated by the light source (ultraviolet (UV), visible, and natural sunlight) with energy greater than its bandgap. This will produce the photo-generated carriers (electrons and holes) which induce the photocatalytic reactions by producing highly reactive radicals such as $O_2^{\bullet-}$, $OH^{\bullet}$, and $HO_2^{\bullet}$, as well as directly degrade the organic pollutants by the process of oxidation [4, 5]. Notably, the surface area of the materials plays a significant role in the photocatalytic reaction since the reaction occurs as the result of the interaction of the photocatalyst with the pollutants through the surface charges. Currently, nano-materials attain widespread research interest as the result of increased surface area which considerably enhances the degradation rate of the pollutants [6].

Nanostructured metal oxide semi-conductors such as TiO_2, SnO_2, $BiVO_4$, ZrO_2, and ZnO are recognized as suitable candidates for photoelectrocatalytic water splitting [7] and photocatalytic applications [8-13] owing to their unique physical and chemical properties. Among the various nanostructured metal oxide semi-conducting materials, ZnO has received

considerable interest owing to its non-toxic nature, high photosensitivity, easy availability, and low cost [14-18]. Various ZnO nanostructures such as nanopowders [19], nanotetrapods [20], nanosheets [21], nanoflowers [22], nanorods (NRs) [23, 24], and nanowires [25] have been utilized as a catalyst for the effective degradation of organic pollutants by the photocatalytic reactions. In general, the nanostructures have been suspended in the organic dye solution for the photocatalytic investigation and its powder form will limit their practical usage due to its complexity in separation and recycling [26]. Also, it is observed that the nanostructured powder will easily aggregate and subsequently reduce its efficiency on the photocatalytic behavior [20, 27]. Instead, ZnO nanostructures synthesized on rigid substrates [28] such as glass, silicon, and sapphire are emerging as the alternate potential approach for the photocatalytic reaction due to numerous benefits including large surface area and reusability. However, the ZnO nanowires fabricated by radio frequency (rf) magnetron sputtering technique are still not investigated for photocatalytic dye degradation analysis. Notably, the ZnO grown by sputtering approach is known to be the better approach to harvesting metal oxide one-dimensional structure with a high degree of uniformity over a large scale without compromising the physio-chemical properties. The reusability of the catalyst for several cycles represents that the ZnO NRs is one of the potential candidates for practical applications as a photocatalyst. In the search for an industrial standard photocatalyst, the analysis of defects is very essential since it will also influence the photocatalytic efficiency by trapping charge carriers on a conduction band generated via absorbing the illuminated light [29].

In the present work, the vertically aligned ZnO NRs have been grown on silicon (111) substrates by the rf-magnetron sputtering technique for photocatalytic dye degradation analysis. This is the maiden report on the photocatalytic activity study of vertically aligned ZnO NRs grown by rf-magnetron sputtering for various organic dye molecules under visible light irradiation. The dye excitation along with the surface defects mediated photo-excitation of electrons is accountable for the enhanced degradation of methylene blue molecules (97%) under solar irradiation.

2. EXPERIMENTAL SECTION

2.1. Fabrication of Vertically Aligned ZnO NRs by rf-Magnetron Sputtering

Vertically aligned ZnO NRs were grown on silicon (111) substrates by rf-magnetron sputtering technique under an argon atmosphere as growth conditions described in the supplementary information [30, 31]. Briefly, the growth was performed under argon deposition pressure of 0.01 mbar for 60 min with the fixed rf power of 60 W. The target-substrate distance and substrate temperature are kept constant as 50 mm and 650° C respectively.

2.2. Characterization of Vertically Aligned ZnO NRs

Morphological analysis was performed using (FESEM, Carl Zeiss-Σigma) equipped with an energy dispersive X-ray (EDX) spectrometer (Oxford instruments-INCAx). The valence state of the ions was characterized by X-ray photoelectron spectroscopy (XPS, Omicron Nano-technology Inc, Germany). Temperature-dependent photoluminescence spectra were recorded by using HORIBA JOBIN YVON monochromator (0.55 m) over the temperature range of 10-300 K with He-Cd laser (wavelength-325 nm and power-30 mW) as the excitation source. The dispersed fluorescence signal from the specimen was collected by a charge-coupled device through a proper optical arrangement.

2.3. Degradation of Various Organic Dye Molecules by ZnO NRs as a Photocatalyst

The photocatalytic activity, efficiency, and photostability of the vertically aligned ZnO NRs grown on Si (111) substrates were investigated from the degradation of organic dyes such as methylene blue (MB), rhodamine B (RhB), and methyl orange (MO) under the irradiation of visible and solar light. The photocatalytic dye declination experiment was performed using ZnO NRs as a catalyst under the natural pH of the dye molecules and its values are 8, 7, and 6.5 for MB, RhB, and MO respectively. Briefly, the volume of 4 ml of 5 mg/L dye solutions was taken in two separate test tubes and 1 x 0.5 cm^2 size of the substrate containing ZnO NRs was immersed into the solution separately. The test tubes were placed at ~16 cm far away from the light source to cancel the heating effect. The irradiation of visible and sunlight was done with a 300 W tungsten halogen lamp (8500 lumens) and natural bright sunlight (12.00 NOON to 4.00 PM) respectively. To reach a stable concentration and adsorption-desorption equilibrium, the dye solution with the catalyst was kept for 30 mins in the dark prior to irradiation. The declination of dye molecules was analysed by recording the UV-Vis absorption spectrum using Shimadzu UV-2450 spectrophotometer at the given interval of time. To examine the photo corrosion and photostability of the vertically aligned ZnO NRs as an efficient catalyst, the photocatalytic declination of MB was repeated for 10 cycles under the illumination of visible light.

3. RESULTS AND DISCUSSION

3.1. Morphological and Optical Studies of ZnO NRs

Figure 1 (a) & (b) show the FESEM images of the vertically aligned ZnO NRs on Si (111) substrates. The average length and diameter of the NRs are measured by using ImageJ processing software and are ascertained to be 0.5 µm and 80 nm respectively. In addition to that, the surface of ZnO NRs is found to be very smooth and densely packed on the substrate with a high degree of uniformity all over the substrate (~5 x 10^9 NRs/cm^2). EDX spectrum of the vertically aligned ZnO NRs represents the existence of zinc, oxygen, and silicon in the sample as shown in Figure S1**.** The structural studies of the ZnO NRs were evaluated using the X-ray diffraction (XRD) analysis and shown in Figure S2. The predominant (002) reflection at ~34.41° with narrow full width at half maximum (FWHM, 660 arcsec) reveals the high crystalline nature with the hexagonal wurtzite crystal structure of the ZnO NRs [32]. The characteristic Raman modes (E_2^{low} and E_2^{high}) at 99.3 and 437.4 cm^{-1} of ZnO NRs (Figure S3) evidence the formation of ZnO and are attributed to the lattice vibrations of zinc and oxygen atoms, respectively [33].

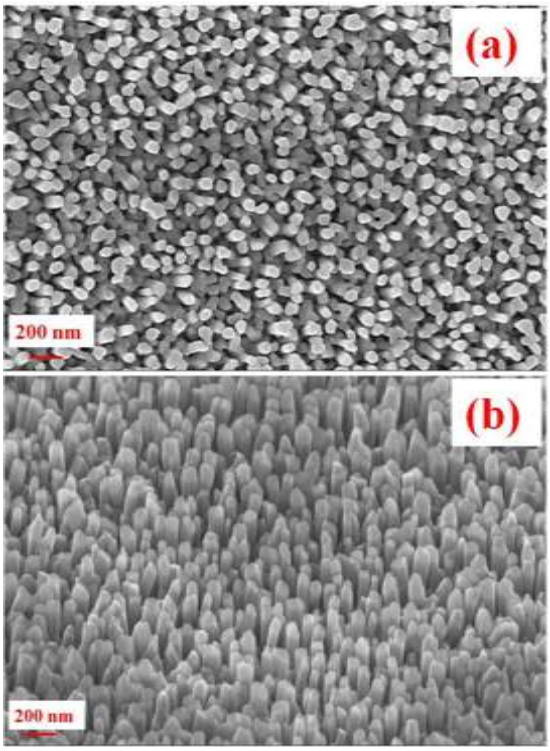

Figure 1. *FESEM images of ZnO NRs grown by rf-magnetron sputtering under a pure argon atmosphere (a) Top view and (b) Tiled view.*

Figure 2 (a)-(d) show the survey scan, Zn 2p, O 1s, and C 1s XPS spectra of the vertically aligned ZnO NRs respectively. XPS survey scan spectrum shown in Figure 2(a), element C is mainly ascribed to the adventitious hydrocarbon from XPS itself as shown in Figure 2(d) [34]. The peaks centred at 1022.8 and 1045.9 eV correspond to the Zn $2p_{3/2}$ and Zn $2p_{1/2}$ chemical states respectively (Figure 2(b)). Importantly, the binding energy separation of the Zn 2p doublet spectral lines is ~23 eV. It is in good agreement with the earlier report [35, 36] and confirms that the zinc ions are in a +2 valence state. The core binding energy region of O 1s possesses the characteristic peaks at 531.3 and 532.8 eV and can be assigned to O-Zn [37] and O^{2-} ions deficient within the matrix of ZnO [38] (Figure 2(c)) respectively. It is clear that the growth of ZnO NRs is performed under a pure argon atmosphere which induces more oxygen vacancies since its formation energy is small compared with other point defects [39]. Further, the relative quantity of oxygen vacancies in ZnO NRs is calculated from the ratio of oxygen-deficient (OD) peak area [OD/O_{Total}] [40] and its value is 49.8%.

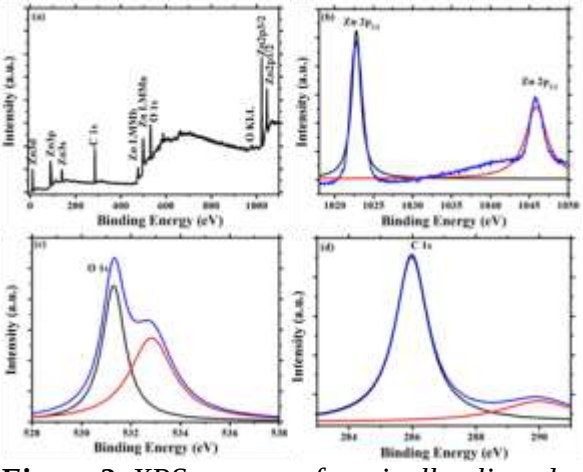

Figure 2. *XPS spectra of vertically aligned ZnO NRs (a) Survey scan spectrum, (b) Zn 2p spectrum, (c) O 1s spectrum, and (d) C 1s spectra.*

In addition to that, the temperature-dependent photoluminescence spectra of vertically aligned ZnO NRs are shown in Figure 3. We observed the dominant emission peak at ~ 3.361 eV and it can be attributed to the neutral donor bound exciton and denoted as D^0X [32]. Notably, the intensity quenching of D^0X emission corroborated to the results of refreezing of phonons with the increase in temperature. Further, a minor peak on the higher energy side of D^0X emission at 3.372 eV corresponds to the free exciton emission and is denoted as FX [32]. It is accounted that the longitudinal optical phonon replicas of ZnO are separated from one another by 71-73 meV [41]. The observed emission peaks at 3.309 and 3.229 eV are associated with the first and second LO phonon replicas of FX emission. Moreover, the additional peak at 3.335 eV is attributed to the two-electron satellite emission as shown in the inset of Figure 3 [32]. In addition to the above peaks, the defect-mediated emissions are observed at 3.01 and 2.192 eV which are corresponding to violet emission (VE) and green emission GE) respectively. These violet and green emissions evidence the existence of zinc and oxygen vacancies in the ZnO NRs [42-45]. It is explained in detail in our earlier work [32].

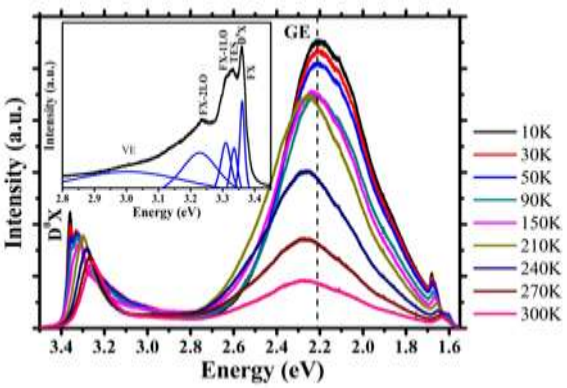

Figure 3. *Temperature - dependent photo-luminescence spectra of vertically aligned ZnO NRs grown on a silicon substrate and the inset of Figure 3 shows the Lorentz fitting of PL for 10 K.*

The D^0X peak energy decreases with increasing the ambient temperature because of the electron-phonon interactions and the lattice dilation. The

shift of the D^0X peak energy is fitted by the well-known empirical Varshni formula (not shown) [46]. It is used to analyze the variation of bandgap energy (E_g) with temperature (T).

$$E(T) = E(0) - \left(\frac{\alpha T^2}{(T + \beta)} \right) \quad (1)$$

where E(T) and E(0) are the bandgaps at an absolute temperature of T and 0 K respectively. α, and β are the Varshni thermal coefficients. The above coefficients are extracted from the best-fitted results of D^0X emission using equation (1). The values of E(0), α, and β for the ZnO NRs are 3.3651 eV, 1.43 meV/K, and 571 K respectively. The obtained values are in accordance with the reported values [47].

3.2. Photocatalytic Studies of Vertically Aligned ZnO NRs

The degradation of the various organic dye molecules such as MB, RhB, and MO is investigated by the photocatalytic behavior of vertically aligned ZnO NRs. Time-dependent UV-Vis absorption spectra of MB, RhB, and MO under the irradiation of visible light have been discussed in supporting information in detail (Figure S4). Notably, the declination percentage of MB, RhB, and MO has been evaluated to be 93.8, 34.1, and 12.6 % respectively under visible light illumination. In order to establish the degradation of the dye molecules induced by the photocatalyst, the percentage of degradation for various organic pollutants under visible light illumination without any catalyst is depicted in Figure S5.

The observation of significant enhancement in the photo-degradation of various dye molecules by ZnO NRs under the irradiation of visible light can be explained with the help of the available mechanism. In general, the degradation of the organic contaminants takes place due to the oxidation and reduction reactions on the surfaces of the photocatalyst. These reduction and oxidation reactions are provoked by the electrons and holes and are generated into the conduction and valence bands respectively by photo-excitation. The separation of electrons and holes is impossible by the irradiation of visible light since the energy is insufficient to excite the electrons from the valence band to the conduction band. Hence, photocatalytic activity is less possible when the catalyst has bandgap energy greater than the excitation energy. However, the defects-induced energy levels within the bandgap of the catalyst can enhance the charge separation and consequently reduce the recombination losses which significantly improves the photocatalytic dye degradation under the illumination of visible light [48]. Further, it is recently reported that if the photocatalyst could not be excited under the illumination of visible light since its bandgap is much higher than the excitation energy, then the organic dye molecules can be excited which induces the photocatalytic reactions by transferring the electrons to the photocatalyst [49]. The photocatalytic declination of organic dye molecules by prepared ZnO NRs under visible light can be demonstrated by the consequences of optical transitions pertaining to the transfer of electrons to photocatalysts or dye molecules. Further, the absorption occurs along the axial direction of the NRs, which is quite long enough for complete light absorption as it efficiently traps the photons by multiple scattering processes by the nanowire geometry, while the charge separation occurs along the radial direction of the NRs.

Under the illumination of visible light, the possibility of the excitation of electrons to the intermediate energy levels induced by the intrinsic point defects is possible due to its adequate excitation energy. The growth conditions play a crucial role in the fabrication of defects-free ZnO NRs since the growth is performed under a pure argon atmosphere. Hence, the formation of intrinsic point defects (oxygen vacancies) is inevitable as the result of insufficient

oxygen free radicals, and further its formation energy is minimum as compared to other point defects. The formation of intrinsic point defects is similar to carrier doping and enhances the light absorption in the visible region. The presence of intrinsic points in the vertically aligned ZnO NRs is evidenced by the temperature-dependent photoluminescence spectra, it is observed that the two defect levels induced by oxygen and zinc vacancies act as donor and acceptor levels within the bandgap of the photocatalyst. The observed oxygen vacancy-mediated donor level lies below the conduction band minimum at ~ 0.5 eV. Therefore, irradiating the catalyst by visible light, the donor and acceptor levels are formed by the oxygen and zinc vacancies respectively which subsequently trap the photo-generated carriers and they easily react with the adsorbed dye molecules on the surface of the ZnO NRs and lead to the formation of highly reactive free radicals. These radicals degrade the organic dye molecules by the processes of oxidation and reduction until a stable neutral species is formed. Consequently, the decolorization of dye will occur under the illumination of visible as well as sunlight. In the above process, the redox reaction occurs on the surface of these defects and mostly by oxygen vacancies since it acts as an active site of the photocatalyst [50].

On the other hand, the catalyst could not be excited under the irradiation of visible light since its bandgap is much higher than the excitation energy. Therefore, the organic dye molecules are excited, the dye acts as a sensitizer of visible light. The excited organic dye molecules become cationic dye radicals by transferring the excited electrons to the electron acceptor (catalyst). Subsequently, the degradation of dye molecules takes place through a reactive oxidation process induced by ZnO NRs.

MB (93.8%) is observed to be highly degraded as compared to RhB (34.1%) and MO (12.6 %) under the irradiation of visible light for 4 hrs. The reason behind the intense variations in performance can be explained by UV-Vis absorption spectra in which MB covers most of the visible region. Hence, a greater number of MB molecules can be excited from the ground state as that of RhB and MO. The excited charge carriers of MB will transfer to the conduction band of ZnO NRs and subsequently generates oxygen peroxide radicals and it directly decomposes the organic pollutants by the effective photocatalytic reaction. It is worth noting that, the standalone pollutant molecules do not degrade when it is illuminated with visible/sunlight since it strongly requires transferring the excited electrons to ZnO NRs which act as a sink for accumulating the generated electrons from the pollutant molecules to produce free radicals. Hence, the degradation of the organic dye molecules is expected to be dominated by the dye excitation along with the surface defects mediated photo-degradation mechanism. A similar degradation mechanism has been witnessed in RhB and MO dye molecules degradation and they are relatively small quantities as compared to MB, this may be attributed to its narrow absorption in the visible region. The photo-degradation of the dye molecules by the ZnO NRs as a catalyst under the illumination of visible light is schematically represented in Scheme 1.

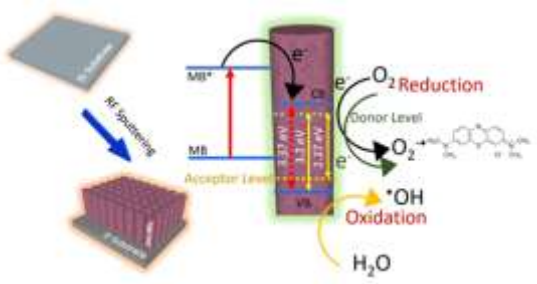

Scheme 1. *A Schematic representation of photocatalytic degradation of dye molecules by the ZnO NRs as a catalyst under visible light irradiation.*

In order to reach a stable dye concentration before irradiation, the

various dye solutions with the photocatalyst were kept under dark conditions for 30 mins. The percentage adsorption of the organic dye molecules on the surface of the catalyst was observed to be 12.7, 7.3, and 2.2 for the MB, RhB, and MO dye molecules respectively. The order of percentage adsorption is MB>RhB>MO which was matched with the percentage degradation of the dye molecules. These results showed that the higher amount of dye molecules on the catalyst surface increases the photocatalytic degradation efficiency which may be due to the transfer of more electrons by the higher amount of excited dye molecules present on the catalyst surface.

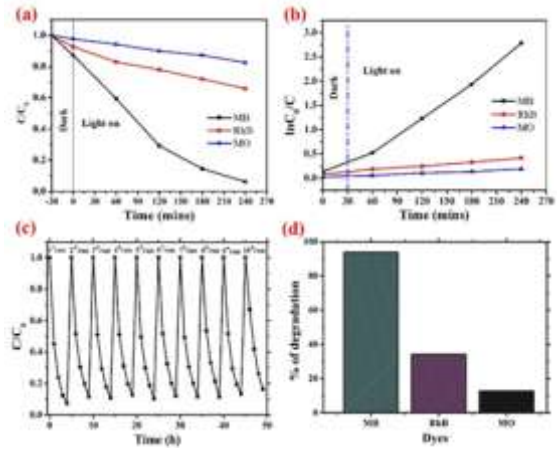

Figure 4. *Photocatalytic dye degradation of ZnO NRs for various organic pollutants under visible light irradiation (a-b) Pseudo first-order kinetic rate plot with respect to irradiation time (c) Reusability test of ZnO NRs for the degradation of MB up to 10 cycles and (d) Historiographic representation of dyes degradation percentage.*

Figure 4 (a) and (b) show the C/C_0 and ln (C_o/C) vs. time curves of the photo-degradation by vertically aligned ZnO NRs as a catalyst under dark and irradiation of visible light. The linear photocatalytic degradation of the organic dye molecules follows the pseudo-first-order reaction kinetics. The equation can be expressed as [4, 51]

$$\ln\left(\frac{C_0}{C}\right) = kt \qquad (2)$$

where C_o is the initial concentration of the dye solution (mol L^{-1}), C is the concentration of the dye solution at time t (mol L^{-1}) and k is the rate constant of the degradation (min^{-1}). The apparent rate constants of various dye molecules are obtained from the best-fitted curves of Eq. (2). The rate constant of ZnO NRs was found to be 0.012, 0.002 and 0.0006 min^{-1} for the MB, RhB, and MO respectively under the illumination of visible light.

Overall, it is suggested that the vertically aligned ZnO NRs can be the potential candidate for the visible light photodegradation of selective organic dye molecules. The proper choice of ZnO NRs grown with necessary doping and appropriate growth condition can be an effective photocatalyst for selective dye degradation. In addition to that, stability is the key to the selection of optimum material for photocatalysts. For this, we have evaluated the photo-stability of ZnO NRs for degradation of the MB dye molecules up to 10 cycles under visible light. At the end of each cycle, the substrate level ZnO NRs were rinsed with de-ionized water to completely remove the organic molecules from the surface of the samples. The stability analysis is depicted in Figure 4 (c), and the results illustrate only a negligible shift in the performance in the 10^{th} cycle as that of the primary cycle which confirms the high ZnO NRs as the catalyst. For visibility, the photostability and non-corrosive nature of degradation percentage of MB, RhB, and MO under irradiation of visible light for 4 hrs is 93.8, 34.1, and 12.6 % respectively as shown in Figure 4 (d).

From the observation, it is noticed that ZnO NRs grown by rf-magnetron sputtering shows the highest first-order kinetics ($K=1.2 \times 10^{-2}$ min^{-1}) as compared with ZnO nanostructures grown by various techniques as given in Table 1. This strongly recommends ZnO NRs for the photocatalytic dye applications of methylene blue.

The degradation of MB dye molecules was explained in detail. MB is a cationic dye and smaller in size which adsorbed highly (12.7 % in dark) on the surface of the catalyst. The C=N and C=S bonds having low dissociation energy present in the MB may result in a higher photocatalytic degradation percentage [56]. The MO is an anionic dye that showed lower adsorption (2.2 % in dark) on the catalyst surface. Moreover, the azo (-N=N-) group present in the MO having high energy of dissociation lower the percentage of photocatalytic degradation [57]. The RhB is a zwitterionic dye having both positively charged (NEt_2) and negatively charged (-COOH) groups which could relatively lower the adsorption as well as the photocatalytic degradation efficiencies than that of MB [58, 59].

Table 1. *Comparison of first-order kinetics of ZnO NRs with other earlier reports of ZnO.*

Photocatalyst	Preparation Method	Light Source	First Order Kinetics, K (min^{-1})	References
ZnO nanoparticle	Microwave Reactor	UV Light (365 nm)	0.65×10^{-2}	[52]
ZnO nanoribbons	Plasma afterglow oxidation process	Xenon Lamp	6.5×10^{-3}	[53]
ZnO nanorods	Precipitation Technique	400 W Tungsten Lamp	1.8×10^{-3}	[54]
ZnO nanomaterials	Sol-Gel Method	150 W Mercury Lamp	0.71×10^{-2}	[55]
ZnO NRs	RF Sputtering	300 W Tungsten Halogen Lamp	1.2×10^{-2}	Present Work

Further, to evaluate the direct implementation of our proposed structure for dye degradation, we have investigated the degradation performance under natural solar illumination. The photocatalytic degradation of MB, RhB, and MO absorption spectra for 0 and 4 hrs of irradiation under solar illumination are shown in Figure 5. ZnO NRs exhibit enhanced photocatalytic decay of 97, 47, and 20% for MB, RhB, and MO respectively under the bright sunlight irradiation for 4 hrs because solar light encompasses the visible spectrum along with a small UV component (~4%). This UV light excites the electrons to the conduction band and leaves holes in the valence band. Hence, the electrons and holes induce photo-degradation through the oxidation and reduction reaction, resulting in high degradation under solar irradiation. The concentration of these electrons and holes on the catalyst under the irradiation of solar light is too small due to the small UV component in the solar spectrum. Therefore, the dye excitation-mediated degradation mechanism and the surface defects play a dominant role under solar irradiation.

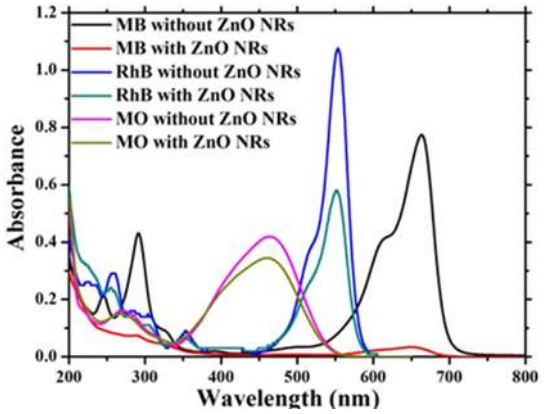

Figure 5. *UV-Vis absorption spectra of various dye molecules in the presence and the absence of vertically aligned ZnO NRs grown on silicon substrate under the irradiation of natural bright sunlight for 4 hrs.*

4. CONCLUSION

We have favourably grown the vertically aligned ZnO NRs on Si (111) substrates by rf-magnetron sputtering. The correlation of temperature-dependent photoluminescence spectra with the photoelectron spectrum of the ZnO NRs confirms the existence of point defects induced by oxygen vacancies. The photocatalytic activity of the ZnO NRs is demonstrated by the degradation of organic dyes under visible and sunlight irradiations. The combined mechanism of dye excitation along with the surface defects mediated photo-excitation of electrons is expected to be responsible for the enhanced decay of MB molecules (97%) under solar irradiation. The photocatalyst is stable (10 cycles) with an almost constant percentage of degradation under visible light irradiation evidencing the practical reusability of ZnO NRs as a standard semiconductor photocatalyst.

ACKNOWLEDGMENT

PSV would like to express his sincere gratitude to the College management and Principal for their generous financial support to develop a Nanomaterials Laboratory. KJ acknowledges DST-FIST, PURSE, and RUSA 2.0 R & I for partial financial support.

CONFLICT OF INTEREST:

We declare that there is no conflict of interest.

REFERENCES

1. Gnanasekar, P., Kulandaivel, J., "Two-dimensional materials for renewable energy devices", *Encyclopedia of Applied Physics,* (2021) 1-39.
2. Mandal, P., Debbarma, J., Saha, M., "Graphene assisted photodegradation of pollutant dyes and its pragmatic effect on lemna minor and eichhornia crassipes", *Int. J. Nanosci. Nanotechnol.,* 18 (2022) 109-122.
3. Raju, S., Ashok, D., Boddu, A. R., "Leucaena leucocephala mediated green synthesis of silver nanoparticles and their antibacterial, dye degradation and antioxidant properties", *Int. J. Nanosci. Nanotechnol.,* 18 (2022) 65-78.
4. Chung, Y. A., Chang, Y. C., Lu, M. Y., Wang, C. Y., Chen, L. J., "Synthesis and photocatalytic activity of small-diameter ZnO nanorods", *J. Electrochem. Soc.,* 156 (2009) 75.
5. Heydari, S., Shirmohammadi Aliakbarkhani, Z., Hosseinpour Zaryabi, M., "Photocatalytic degradation of safranin dye from aqueous solution using nickel nanoparticles synthesized by plant ,leaves"*Int. J. Nanosci. Nanotechnol.,* 16 (2020) 153-165.
6. Anaraki Firooz, A., Keyhani, M., "The effect of different dopants (Cr, Mn, on (Cu and Ni ,Co ,Fe photocatalytic ,properties of ZnO nanostructures"*Int. J. Nanosci. Nanotechnol.,* 16 (2020) 59-65.
7. Maeda, K., Teramura, K., Lu, D., Saito, N., Inoue, Y., Domen, K., "Noble-metal/Cr_2O_3 core/shell nanoparticles as a cocatalyst for photocatalytic overall water splitting", *Angew. Chem., Int. Ed.,* 45 (2006) 7806-7809.
8. Zheng, Y., Chen, C., Zhan, Y., Lin, X., Zheng, Q., Wei, K., Zhu, J., Zhu, Y., "Luminescence and photocatalytic activity of ZnO nanocrystals: correlation between structure and property", *Inorg. Chem.,* 46 (2007) 6675-6682.
9. Kumar, S. G., Devi, L. G., "Review on modified TiO_2 photocatalysis under UV/visible light: selected results and related mechanisms on interfacial charge carrier transfer dynamics", *J. Phys. Chem.,* 115 (2011) 13211-13241.
10. Ganeshbabu, M., Kannan, N., Sundara Venkatesh, P., Paulraj, G., Jeganathan, K., Mubarak Ali, D., "Synthesis and characterization of $BiVO_4$ nanoparticles for environmental applications", *RSC Adv.,* 10 (2020) 18315-18332.
11. Vijayalakshmi, S., Kumar, E., Sundara Venkatesh, P., Raja, A., "Preparation of zirconium oxide with polyaniline nanocatalyst for the decomposition of pharmaceutical industrial wastewater", *Ionics,* 26 (2020) 1507-1513.
12. Vijayalakshmi, S., Kumar, E., Ganeshbabu, M., Sundara Venkatesh, P., Rathnakumar, K., "Structural, electrical, and photocatalytic investigations of PANI/ZnO nanocomposites", *Ionics,* 27 (2021) 2967-2977.
13. Pal, S., Mondal, S., Maity, J., Mukherjee, R., "Synthesis and characterization of ZnO nanoparticles using Moringa Oleifera leaf extract: investigation of photocatalytic and antibacterial activity", *Int. J. Nanosci. Nanotechnol.,* 14 (2018) 111-119.

14. Rehman, S., Ullah, R., Butt, A. M., Gohar, N. D., "Strategies of making TiO_2 and ZnO visible light active", *J. Hazard. Mater.,* 170 (2009) 560-569.
15. Di Paola, A., García-López, E., Marcì, G., Palmisano, L., "A survey of photocatalytic materials for environmental remediation", *J. Hazard. Mater.,* 211 (2012) 3-29.
16. Lam, S. M., Sin, J. C., Abdullah, A. Z., Mohamed, A. R., "Degradation of wastewaters containing organic dyes photocatalyzed by zinc oxide A review", *Desalin. Water. Treat.,* 41 (2012) 131-169.
17. Djurisic, A. B., Chen, X., Leung, Y. H., Ng, A. M. C., "ZnO nanostructures: growth, properties, and applications", *J. Mater. Chem.,* 22 (2012) 6526-6535.
18. Portela, R., Hernández-Alonso, M. D., "Environmental applications of photocatalysis", *Green Energy Technol.,* 71 (2013) 35-66.
19. Kaur, J., Bansal, S., Singhal, S., "Photocatalytic degradation of methyl orange using ZnO nanopowders synthesized via thermal decomposition of oxalate precursor method", *Physica B Condens.,* 416 (2013) 33-38.
20. Wan, Q., Wang, T. H., Zhao, J. C., "Enhanced photocatalytic activity of ZnO nanotetrapods", *Appl. Phys. Lett.,* 87 (2005) 083105.
21. Zhang, D., Liu, X., Wang, X., "Growth and photocatalytic activity of ZnO nanosheets stabilized by Ag nanoparticles", *J. Alloys Compd.,* 509 (2011) 4972-4977.
22. Wang, Y., Li, X., Wang, N., Quan, X., Chen, Y., "Controllable synthesis of ZnO nanoflowers and their morphology-dependent photocatalytic activities", *Sep. Purif. Technol.,* 62(3) (2008) 727-732.
23. Baruah, S., Jaisai, M., Imani, R., Nazhad, M. M., Dutta, J., "Photocatalytic paper using zinc oxide nanorods", Sci. Technol. *Adv. Mater.,* 11(5) (2010) 055002.
24. Leelavathi, A., Madras, G., Ravishankar, N., "Origin of enhanced photocatalytic activity and photoconduction in high aspect ratio ZnO nanorods", *Phys. Chem. Chem. Phys.,* 15 (2013) 10795-10802.
25. Kuo, T. J., Lin, C. N., Kuo, C. L., Huang, M. H., "Growth of ultralong ZnO nanowires on silicon substrates by vapor transport and their use as recyclable photocatalysts", *Chem. Mater.,* 19 (2007) 5143-5147.
26. Xie, Y., Yuan, C., "Transparent TiO_2 sol nanocrystallites mediated homogeneous-like photocatalytic reaction and hydrosol recycling process", J. Mater. Sci., 40 (2005) 6375-6383.
27. Liu, H., Yang, J., Liang, J., Huang, Y., Tang, C., "ZnO nanofiber and nanoparticle synthesized through electrospinning and their photocatalytic activity under visible light", *J. Am. Ceram.,* 91 (2008) 1287-1291.
28. Yang, J. L., An, S. J., Park, W. I., Yi, G. C., Choi, W., "Photocatalysis using ZnO thin films and nanoneedles grown by metal-organic chemical vapor deposition", *Adv. Mater.,* 16 (2004) 1661-1664.
29. Maness, P. C., Smolinski, S., Blake, D. M., Huang, Z., Wolfrum, E. J., Jacoby, W. A., "Bactericidal activity of photocatalytic TiO_2 reaction: toward an understanding of its killing mechanism", *Appl. Environ. Microbiol.,* 65 (1999) 4094-4098.
30. Sundara Venkatesh, P., Purushothaman, V., Esakki Muthu, S., Arumugam, S., Ramakrishnan, V., Jeganathan, K., Ramamurthi, K., "Role of point defects on the enhancement of room temperature ferromagnetism in ZnO nanorods", *Cryst. Eng. Comm.,* 14 (2012) 4713-4718.
31. Sundara Venkatesh, P., Jeganathan, K., "Investigations on the growth and characterization of vertically aligned zinc oxide nanowires by radio frequency magnetron sputtering", *J. Solid State Chem,,* 200 (2013) 84-89.
32. Sundara Venkatesh, P., Jeganathan, K., "Investigations on the morphological evolution of zinc oxide nanostructures and their optical properties", *CrystEngComm.,* 16 (2014) 7426.
33. Sundara Venkatesh, P., Ramakrishnan, V., Jeganathan, K., "Investigations on the growth of manifold morphologies and optical properties of ZnO nanostructures grown by radio frequency magnetron sputtering", *AIP Advances,* 3 (2013) 082133.
34. Wang, H. L., Ding, W. Y., Liu, C. Q., Chai, W. P., "Influence of O_2 flux on compositions and properties of ITO films deposited at room temperature by direct-current pulse magnetron sputtering", *Chin. Phys. Lett.,* 27 (2010) 127302.
35. Gao, D., Zhang, J., Yang, G., Zhang, J., Shi, Z., Qi, J., Zhang, Z., Xue, D., "Ferromagnetism in ZnO Nanoparticles Induced by Doping of a Nonmagnetic Element", *J. Phys. Chem. C.,* 114 (2010) 13477-13481.
36. Sundara Venkatesh, P., Balakumar, S., Jeganathan, K., "Post-annealing effects on the structural and optical properties of vertically aligned undoped ZnO nanorods grown by radio frequency magnetron sputtering", *RSC Adv.,* 4 (2014) 5030-5035.
37. Coppa, B. J., Davis, R. F., Nemanich, R. J., "Gold Schottky contacts on oxygen plasma-treated, n-type ZnO(000Ī)", *Appl. Phys. Lett.,* 82 (2003) 400.
38. Chen, M., Pei, Z. L., Wang, X., Yu, Y. H., Liu, X. H,. Sun, C., Wen, L. S., "Intrinsic limit of electrical properties of transparent conductive oxide films", *J. Phys. D: Appl. Phys.,* 33 (2000) 2538-2548.
39. Kim, Y., Kang, S., "Calculation of Formation Energy of Oxygen Vacancy in ZnO Based on Photoluminescence Measurements", *J. Phys. Chem. B.,* 114 (2010) 7874-7878.

40. Hyung Kim, D., Youn Yoo, D., Kwang Jung, H., Hwan Kim, D., Yeol Lee, S., "Origin of instability by positive bias stress in amorphous Si-In-Zn-O thin film transistor", *Appl. Phys. Lett.,* 99 (2011) 2009.
41. Özgür, Ü., Alivov, Y. I., Liu, C., Teke, A., Reshchikov, M. A., Dogan, S., Avrutin, V., Cho, S. J., Morkoc, H., "A comprehensive review of ZnO materials and devices", *J. Appl. Phys.,* 98 (2005) 041301.
42. Vanheusden, K., Seager, C. H., Warren, W. L., Tallant, D. R., Voigt, J. A., "Correlation between photoluminescence and oxygen vacancies in ZnO phosphors", *Appl. Phys. Lett.,* 68 (1996) 403.
43. Fang, Z., Wang, Y., Xu, D., Tan, Y., Liu, X., "Blue luminescent center in ZnO films deposited on silicon substrates", *Optical Materials,* 26 (2004) 239-242.
44. Cao, B., Cai, W., Zeng, H., "Temperature-dependent shifts of three emission bands for ZnO nanoneedle arrays", *Appl. Phys. Lett.,* 88 (2006) 161101.
45. Liu, H., Zeng, F., Lin, Y., Wang, G., Pan, F., "Correlation of oxygen vacancy variations to band gap changes in epitaxial ZnO thin films", *Appl. Phys. Lett.,* 102 (2013) 181908.
46. Varshni, Y. P., "Temperature dependence of the energy gap in semiconductors", *Physica,* 34 (1967) 149-154.
47. Alvi, N. H., Riaz, M., Tzamalis, G., Nur, O., Willander, M., "Junction temperature in n-ZnO nanorods/(p-4H-SiC, p-GaN, and p-Si) heterojunction light-emitting diodes", *Solid State Electron.,* 54 (2010) 536-540.
48. Wang, J., Liu, P., Fu, X., Li, Z., Han, W., Wang, X., "Relationship between oxygen defects and the photocatalytic property of ZnO nanocrystals in Nafion membranes", *Langmuir*, 25 (2009) 1218-1223.
49. Wang, B., Li, C., Cui, H., Zhang, J., Zhai, J., Li, Q., "Fabrication and enhanced visible-light photocatalytic activity of Pt-deposited TiO_2 hollow nanospheres", *Chem. Eng. J.*, 223 (2013) 592-603.
50. Baruah, S., Mahmood, M. A., Myint, M. T. Z., Bora, T., Dutta, J., "Enhanced visible light photocatalysis through fast crystallization of zinc oxide nanorods", *Beilstein J. Nanotechnol.,* 1 (2010) 14–20.
51. Bao, N., Feng, X., Yang, Z., Shen, L., Lu, X., "Highly Efficient Liquid-Phase Photooxidation of an Azo Dye Methyl Orange over Novel Nanostructured Porous Titanate-Based Fiber of Self-Supported Radially Aligned $H_2Ti_8O_{17}{\cdot}1.5H_2O$ Nanorods", *Environ. Sci. Technol.,* 38 (2004) 2729-2736.
52. Długosz, O., Banach, M., "Continuous synthesis of photocatalytic nanoparticles of pure ZnO and ZnO modified with metal nanoparticles", *J. Nanostructure Chem.,* 11 (2021) 601-617.
53. Perez, T., Imam, A., Pilloud, D., Ghanbaja, J., Miska, P., Belmonte, T., Gries, T., "Tunable morphologies of ultrathin ZnO nanostructures synthesized by a plasma afterglow-assisted oxidation process and their photocatalytic properties", *Plasma Sources Sci. Technol.,* 28 (2019) 045008.
54. Rabbani, M., Shokraiyan, J., Rahimi, R., Amrollahi, R., "Comparison of photocatalytic activity of ZnO, Ag-ZnO, Cu-ZnO, Ag, Cu-ZnO and TPPS/ZnO for the degradation of methylene blue under UV and visible light irradiation", *Water Sci. Technol.,* 84 (2021) 1813-1825.
55. Isai, K. A., Shrivastava, V. S., "Photocatalytic degradation of methylene blue using ZnO and 2%Fe–ZnO semiconductor nanomaterials synthesized by sol-gel method: a comparative study", *SN Appl. Sci.,* 1 (2019)1247.
56. Li, Y-F., Zhang, W-P., Li, X., Yu, Y., "TiO_2 nanoparticles with high ability for selective adsorption and photodegradation of textile dyes under visible light by feasible preparation", *J. Phys. Chem. Solids*, 75 (2014) 86-63.
57. Ariyanti, D., Maillot, M., Gao, W., "Photo-assisted degradation of dyes in a binary system using TiO_2 under simulated solar radiation", *J. Environ. Chem. Eng.,* 6 (2018) 539-548.
58. Verma, S., Tirumala Rao, B., Singh, R., Kaul, R., "Photocatalytic degradation kinetics of cationic and anionic dyes using Au–ZnO nanorods: Role of pH for selective and simultaneous degradation of binary dye mixtures", *Ceram. Int.,* 47 (2021) 34751-34764.
59. Divya, B., Karthikeyan, C., Rajasimman, M., "Chemical synthesis of zinc oxide nanoparticles and its application of dye decolourization", *Int. J. Nanosci. Nanotechnol.,* 14 (2018) 267 - 275.